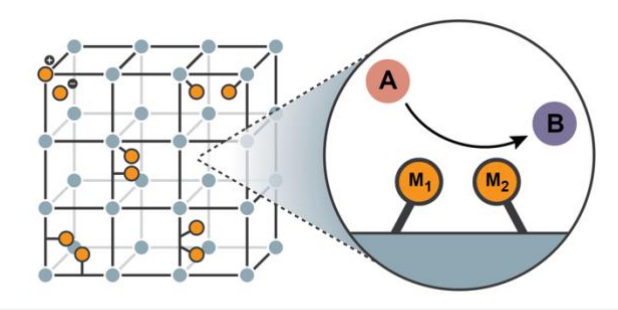
Engineering Bimetallic Active Sites in Metal-Organic Frameworks: Challenges and Opportunities

Jackson Geary,^a Dianne J. Xiao^{a*}

^aDepartment of Chemistry, University of Washington, Seattle, Washington 98195, United States

Abstract

Examples of two metal centers working synergistically to catalyze challenging chemical transformations can be found throughout biological and synthetic systems. In each case, specific metal identities, ligand environments, and metal–metal distances are required. The structural precision needed to engineer a productive, surface-supported



bimetallic active sites in metal-organic frameworks

bimetallic active site represents an opportunity for metal—organic frameworks. In this perspective, we summarize the different ways binuclear metal active sites have been synthesized in metal—organic frameworks and applied in catalysis. Selected examples from the literature will be highlighted to illustrate both the diversity of synthetic approaches as well as the diversity of bimetallic structures.

1 Introduction

Binuclear metal active sites can be found throughout all subfields of catalysis, from homogeneous and heterogeneous systems to enzymes. The mechanisms by which two metal centers may interact synergistically are as rich and varied as the diverse bimetallic structures that have been synthesized in the laboratory and evolved in biology. For example, two redox-active metals can work together to share the redox load of demanding multi-electron transformations. ^{1–4} Similarly, redox-inactive metal centers can cooperatively bind and orient reaction partners, enhancing their local concentration, electrophilicity, and/or nucleophilicity. ^{5–7} In other cases, the second metal may have no direct interaction with the substrate(s), but serves a critical role in modulating the reactivity of its partner. ^{8,9} While an exhaustive discussion of the different classes of bimetallic catalysis is beyond the scope of this perspective, these selected examples underscore the diversity of bimetallic structures and catalytic mechanisms.

Even from the brief overview outlined above, it is evident that different bimetallic mechanisms require different metal identities, ligand environments, and metal-metal distances. *Thus, both structural precision and tunability are key to engineering productive bimetallic catalysts*. While these structural parameters are easily controlled in enzymes and molecular catalysts, comparable synthetic control is more difficult to achieve in a heterogeneous platform. However, while the synthetic barriers are high, the potential pay-off is also considerable. Heterogeneous supports

^{*}Corresponding author: djxiao@uw.edu

allow researchers to explore unique catalyst design parameters, including site isolation, highly constrained geometries, pore confinement, and microenvironment effects. 10–15

As crystalline porous solids built from metal nodes connected by bridging organic linkers, metal–organic frameworks (MOFs) maximize both structural precision and chemical tunability. From this perspective, MOFs are an ideal platform for investigating bimetallic motifs in a heterogeneous context. Indeed, many of the cooperative mechanisms observed in enzymes, molecular catalysts, and heterogeneous systems have been implemented in MOFs (**Fig. 1**). For example, redox-active diiron and dicopper pairs have been explored in MOFs for methane oxidation, ^{16–18} and diiron sites have been studied for photochemical H₂ production. ^{19,20} Redoxinactive pairs have also been investigated, such as Zr(IV) and Zn(II) sites for CO₂ hydrogenation to methanol. ²¹ Finally, bimetallic sites containing one redox-active and one redox-inactive metal have also been designed, such as the pairing of anionic [Co(CO)₄]⁻ complexes and Lewis acidic metal nodes for epoxide and β-lactone carbonylation (**Fig. 1**). ^{22,23}

In this perspective, we summarize the different ways researchers have approached the synthesis of bimetallic active sites in metal—organic frameworks and discuss of the strengths and limitations of each method. Finally, we conclude with an outlook on the challenges and opportunities in MOF-supported bimetallic catalysis.

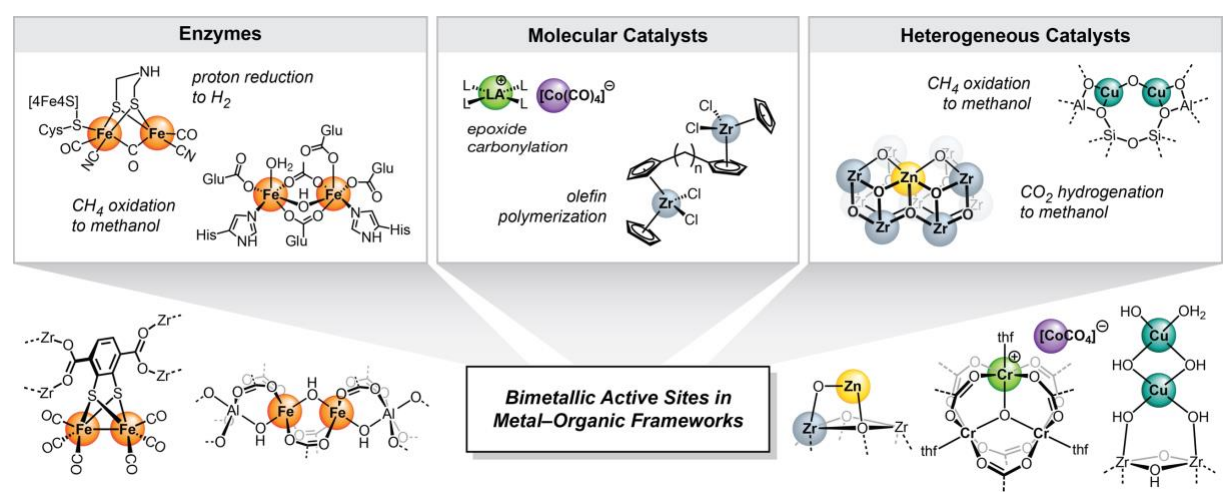


Fig. 1 | Overview of bimetallic active sites in biological and synthetic systems. *Top:* Selected examples of bimetallic active sites in enzymes, molecular complexes, and heterogeneous systems, based off references 1–4, 5–7, 10, and 15. *Bottom:* Overview of how these bimetallic active sites have been replicated in metal–organic frameworks, based off references 16–23.

1.1 Scope and aims

The aim of this perspective is to introduce readers to the different ways binuclear metal active sites have been synthesized in metal—organic frameworks. Selected examples from the literature will be used to illustrate both the diversity of synthetic approaches as well as the diversity of bimetallic structures that can be obtained. While catalytic applications will be touched upon briefly within the context of each example, more comprehensive discussions on MOF catalysis can be found elsewhere, 12,24,25 including focused reviews on MOF electrocatalysis 26–28 and

photocatalysis.^{29–31} Furthermore, our discussion will be restricted to well-defined active sites where the two metal centers are colocalized within the same pore. Thus, we will not discuss systems where the metals are more spatially separated, such as core–shell structures,^{32–36} or systems that are less molecularly defined, such as MOF-derived amorphous materials^{36–39} and MOF-supported bimetallic nanoparticles.^{40,41} Finally, while there are several elegant examples of using cooperative metal–metal interactions to enhance gas sorption,^{42–44} the emphasis here will be on the use of bimetallic sites for reactivity and catalysis. We encourage readers interested in these areas to consult the articles and reviews cited above.

2 Synthetic strategies

An overview of the strategies researchers have used to achieve two proximal metal centers in MOFs is provided in **Fig. 2**. The different synthetic methods can be broadly divided into two categories: 1) the use of multinuclear metal nodes directly for catalysis (<u>Section 2.1</u>), and 2) surface grafting approaches, where bimetallic sites are anchored to the pore walls (<u>Sections 2.2</u>–2.4). The grafting approaches can be further subdivided according to where the metal center is attached, such as at the metal node (<u>2.2</u>), ligand strut (<u>2.3</u>), or a combination of the two (<u>2.4</u>).

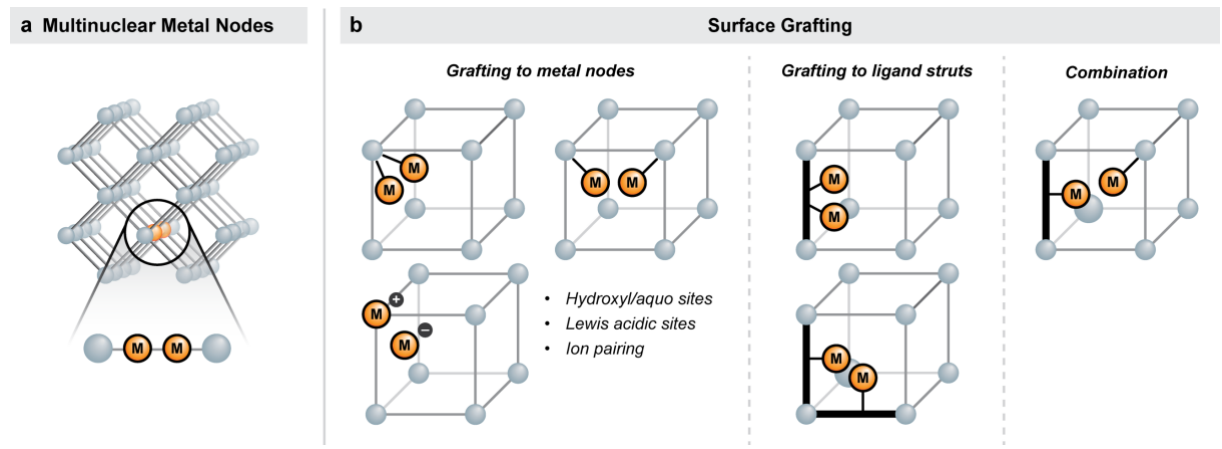


Fig. 2 | Overview of strategies to incorporate bimetallic active sites in metal—organic frameworks. Examples include (a) the direct use of multinuclear metal nodes and (b) surface grafting strategies: grafting to metal nodes, grafting to ligand struts, and combinatorial approaches.

2.1 Multinuclear metal nodes

In many metal—organic frameworks, the inorganic building blocks are not isolated monomeric metal cations, but rather multinuclear metal clusters or even infinite 1D metal—ligand chains. These clusters and chains can serve directly as binuclear or multinuclear active sites for catalysis, either in single metal or mixed-metal variants (**Figs. 3** and **4**). While this approach affords somewhat lower chemical tunability, as it is limited to the structures of existing metal nodes, the advantage of this approach lies in its relative synthetic ease. Bimetallic active sites can often be obtained directly upon MOF formation, with no additional post-synthetic modifications required.

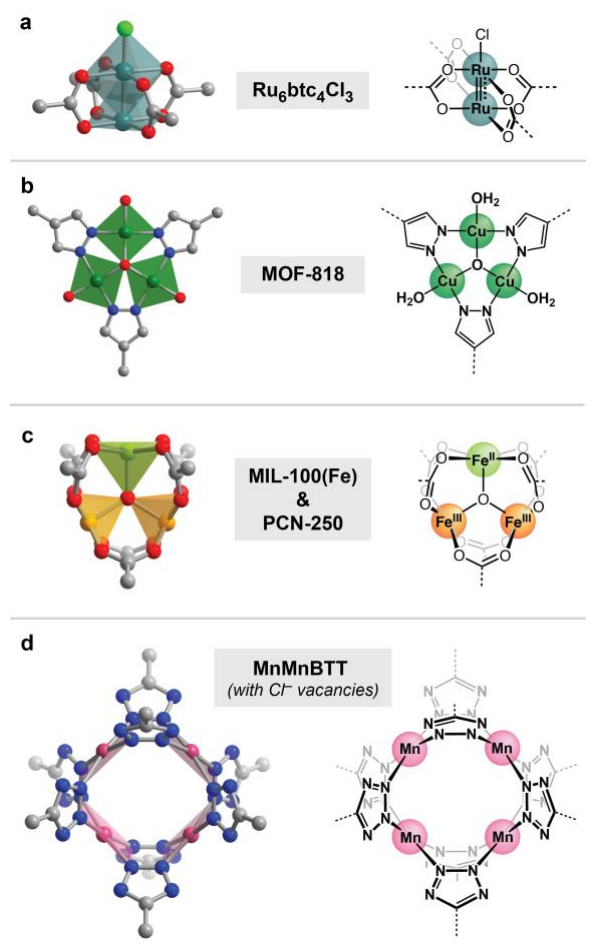


Fig. 3 | Multinuclear MOF nodes, including (a) diruthenium sites for C–H amination, (b) trinuclear copper clusters for aerobic catechol oxidation, (c) trinuclear iron(II)/(III) clusters for methane oxidation, and (d) tetranuclear manganese sites for reversible O_2 cleavage. Figures based off references 45, 47, 49, and 51

upon framework activation (Fig. 3c). 49,50

2.1.1 Multinuclear clusters

Frameworks containing redox-active biand multinuclear cluster-based nodes have been used to facilitate challenging multielectron processes, both stoichiometrically and catalytically (Fig. 3). For example, Powers and coworkers have studied C-H amination in $(btc^{3-}$ Ru6btc4Cl3 benzene-1,3,5tricarboxylate). a framework containing dimeric Ru₂(II/III) nodes (Fig. 3a). The axial chloride bound to each dimer was replaced with N₃⁻ and used to carry out the stoichiometric conversion of toluene to benzylamine. 45,46

Redox-active trinuclear metal nodes have also been explored for oxidative reactions. One example is MOF-818, which contains trinuclear copper(II) nodes with three open coordination sites (typically bound by water or solvent) (Fig. 3b).⁴⁷ These tricopper centers have been explored as catalysts for bio-inspired catechol oxidation using O2.48 Similarly, the trinuclear iron nodes in MIL-100(Fe) (MIL = Materials of Institute Lavoisier) and PCN-250 (PCN = Porous Coordination Network) have been investigated for the stoichiometric oxidation of methane to methanol in the presence of N₂O. In these frameworks, the reactivity is attributed to the one coordinatively unsaturated Fe(II) site per cluster that forms

Finally, intriguing stoichiometric O₂ reactivity has been observed in the framework MnMnBTT (MnMnBTT = Mn₃[(Mn₄Cl)₃BTT₈]₂, BTT³⁻ = 1,3,5-benzenetristetrazolate), which is constructed from tetranuclear [Mn₄Cl]⁷⁺ nodes.⁵¹ Recently, Dincă and coworkers discovered that a portion of the bridging chlorides can be removed post-synthetically, leaving behind an unusual cavity with four inward-oriented open metal sites (**Fig. 3d**). By distributing the redox burden across four metals, these square-planar tetramanganese clusters are able to reversibly cleave and re-form the O–O bonds in O₂, a challenging 4 e⁻ process.⁵² This example nicely highlights how the structural rigidity of MOFs allows the formation of unusual metal arrangements and geometries that would be difficult to achieve otherwise.

2.1.2 1D chains

The short intermetal distances and strong metal–metal communication in frameworks constructed from infinite 1D metal–ligand chains have been leveraged to cooperatively bind molecules such as CO₂ and CO.^{42,43} In addition to gas separation applications, such systems have also been investigated for cooperative reactivity. For example, Wade and coworkers synthesized Fe(bppdi)(DMF)_{0.5} (H₂bppdi = 2,6-bis(1H-pyrazolyl)pyromellitic diimide), a framework containing 1D chains of coordinatively unsaturated Fe(II) centers, and showed it could be used to carry out the stoichiometric reduction of NO to N₂O (**Fig. 4a**).⁵³

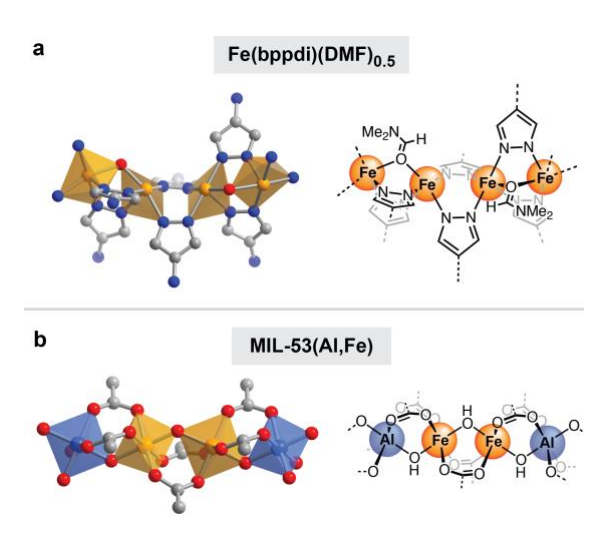


Fig. 4 | Frameworks containing 1D chains, including (a) Fe(bppdi)(DMF)_{0.5}, a framework containing coordinatively unsaturated Fe(II)-pyrazolate centers, and (b) electrochemically synthesized MIL-53(Al,Fe). Figures based off references 53 and 16.

In addition to using the monometallic frameworks directly, researchers have also explored the use of mixed-metal frameworks to achieve site-isolated bimetallic species within an extended 1D chain. One example of efforts in this area is the work by Pidko, Gascon, and coworkers on the MIL-53 structure, 16 which has M(OH)bdc ($bdc^{2-} = 1.4$ formula benzenedicarboxylate). 54-57 The framework is composed of infinite chains of corner-sharing M³⁺ octahedra bridged by bdc²⁻ and hydroxide ligands to generate a framework with diamondone-dimensional channels. shaped Gascon, and coworkers proposed that isolated monomeric and dimeric Fe(III) centers could be achieved in the electrochemically synthesized mixed-metal framework MIL-53(Al,Fe), which contains a mixture of Al(III) and Fe(III) sites

(**Fig. 4b**). ¹⁶ The researchers showed that the mixed-metal system catalyzed the selective oxidation of methane using H₂O₂ as the oxidant, with a combined selectivity for oxygenates (MeOH, MeOOH and formic acid) of ~80%. Spectroscopic methods such as Mössbauer spectroscopy suggested the presence of both isolated, monomeric Fe(III) sites and antiferromagnetically coupled Fe(III)–Fe(III) dimers, though longer chain oligomers cannot be ruled out based on the spectroscopic evidence provided.

The distribution of monomeric, dimeric and potentially oligomeric active sites in MIL-53(Al,Fe) highlights the main shortcoming of mixed-metal frameworks: controlling active site nuclearity. While the overall metal composition is readily tuned, the spatial distribution of metal cations is not. However, Gándara and coworkers recently showed that pre-formed molecular clusters can be used to control the relative arrangement of metals in mixed-metal MOFs. ⁵⁸ As such strategies mature, they may become promising routes to achieve the selective synthesis of site-isolated bimetallic species in mixed-metal frameworks.

2.2 Grafting to metal nodes

The surfaces of metal nodes often feature reactive functional groups, such as Brønsted acidic hydroxyl/aquo ligands, Lewis acidic metal centers, and loosely bound counterions. The chemistry of these reactive groups can be leveraged to attach additional metal centers via covalent bonds, coordination bonds, and electrostatic interactions. While many of these procedures were originally developed in the context of grafting mononuclear metal complexes, they have since been adapted to achieve bimetallic active sites.

The majority of MOFs that have been explored for grafting at the metal node are constructed from highly oxophilic metals (e.g., Ti⁴⁺, Zr⁴⁺, and Hf⁴⁺). The polynuclear metal oxide clusters found in these structures have both high chemical stability as well as rich surface chemistry (**Fig.** 5).⁵⁹ For example, these metal oxide clusters are often decorated with surface hydroxyl and aquo groups, which can be deprotonated and used to anchor additional metal cations (Section 2.2.1). Similarly, dangling surface monocarboxylates can be exchanged for ditopic ligands that can react with additional metal cations (Section 2.2.2). Finally, charged metal nodes with loosely bound counterions can be used to tether oppositely charged metal complexes through ion pairing (Section 2.2.3).

2.2.1 Anchoring to surface hydroxyl/aquo groups

The use of surface hydroxyl/aquo groups to anchor organometallic species and other metal complexes has been most extensively explored in zirconium-based frameworks. The structures of three representative zirconium frameworks, UiO-66 (UiO = University of Oslo),⁶⁰ NU-1000 (NU = Northwestern University),⁶¹ and MOF-808,⁶² are illustrated in **Fig. 5**. While the nodes of all

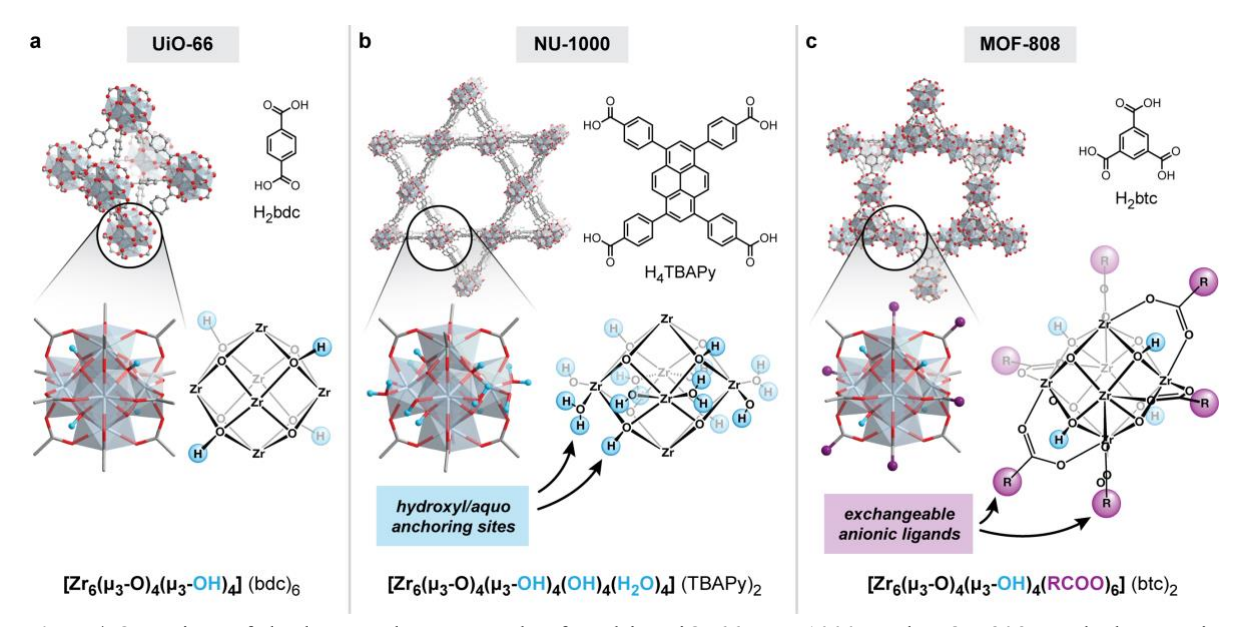


Fig. 5 | Overview of the hexanuclear Zr_6 nodes found in UiO-66, NU-1000, and MOF-808. Both the reactive Brønsted acidic hydroxyl/aquo groups, as well as the dangling anionic ligands attached to Lewis acidic Zr^{4+} sites, can be used as attachment points for grafting additional metals. For clarity, the bridging ligand struts are omitted in the Lewis structure depictions of the Zr_6 nodes. Figures based off references 60, 61, and 62.

three frameworks share the same hexanuclear $Zr_6(\mu_3-O)_4(\mu_3-OH)_4$ core, the clusters differ in the number of bound bridging ligands. For example, the nodes in UiO-66 are 12-connected (i.e., bound by 12 ligand struts, see **Fig. 5a**), to give an overall formula of $Zr_6O_4(OH)_4(bdc)_6$ ($bdc^{2-} = 1,4$ -benzenedicarboxylate). On the other hand, the nodes of NU-1000 and MOF-808 are 8- and 6-connected, respectively. In NU-1000, the excess charge of the cluster and open coordination sites are balanced by additional hydroxide (4×) and water molecules (4×) to give an overall formula of $Zr_6O_4(OH)_8(H_2O)_4(TBAPy)_2$ ($TBAPy^{4-} = 4,4',4'',4'''$ -(pyrene-1,3,6,8-tetrayl)tetrabenzoate) (**Fig.**

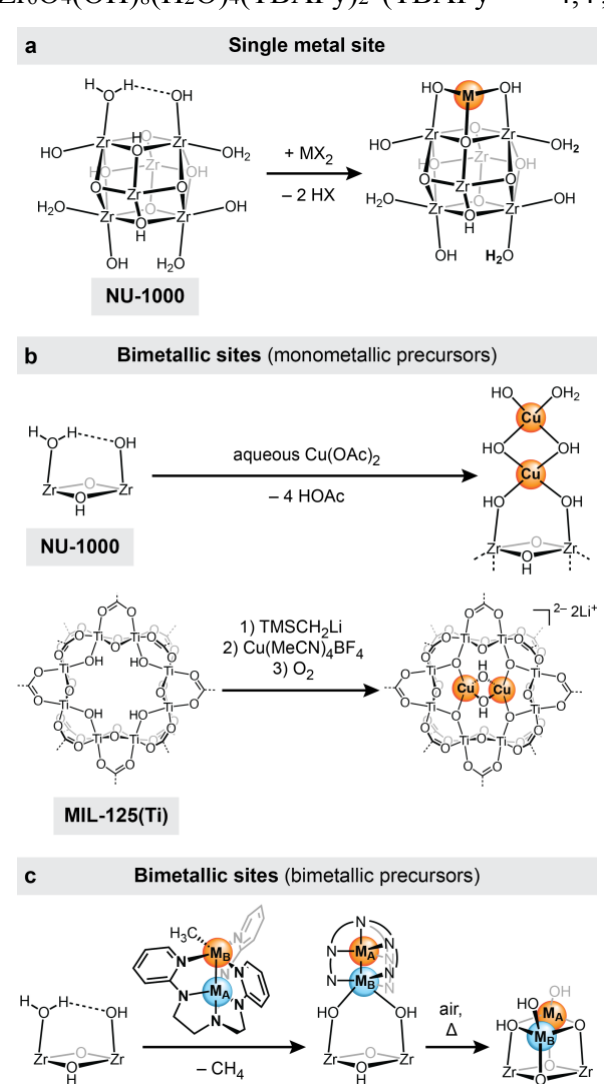


Fig. 6 | Grafting metal centers to the surface hydroxyl species in NU-1000 and MIL-125(Ti). In principle, this strategy can be used to install (a) monometallic sites, (b) bimetallic sites using mononuclear precursors, and (c) bimetallic sites using preformed binuclear complexes. Figures based off references 61, 18, 69, and 70.

NU-1000

M_A = Al(III) M_B = Co(II) **5b**). In MOF-808, the remaining charge and coordination sites are balanced by six additional monoanionic ligands (e.g., a monocarboxylate RCOO⁻, such as acetate or formate) to give the overall formula unit $Zr_6O_4(OH)_4(RCOO)_6(btc)_2$ (btc³⁻ = 1,3,5-benzenetricarboxylate) (**Fig. 5c**).

Farha, Hupp, and coworkers were among the first to recognize that these zirconium nodes could be used as grafting sites. In 2013, they reported the gas-phase metalation of NU-1000 reactive with organometallic complexes.⁶¹ In a procedure analogous to atomic layer deposition (ALD), NU-1000 was exposed to volatile organometallic precursors such as AlMe₃ and ZnEt₂ in the gas-phase, which led to the deprotonation of the surfacebound hydroxyl/aquo ligands and subsequent metalation (Fig. 6a). The strategy, named atomic layer deposition in metal-organic frameworks (AIM), was later extended to other volatile organometallic precursors, including InMe₃ and metal bis(amidinate) complexes (M(II) = Ni, Co, Cu). ^{63–66} Conceptually similar approaches have also been developed for solution-phase metalation. For example, Lin and coworkers showed that the hydroxyl groups in UiO-68, the terphenyl-expanded analogue of UiO-66, can be deprotonated using nBuLi.⁶⁷ Subsequent salt metathesis with MX₂ salts (e.g., CoCl₂, FeBr₂) can be used to quantitatively achieve mononuclear transition metal active sites. Wang and coworkers extended this strategy to MOF-808.²¹ They used ZnEt₂ to simultaneously deprotonate and metalate the four surface hydroxyl groups with Zn(II), creating Zn–Zr sites for CO₂ hydrogenation.²¹

A major challenge in extending this grafting approach from mononuclear sites to binuclear sites is controlling and characterizing active site nuclearity. As the metal loading increases, the speciation of active sites becomes more difficult to control and can even vary depending on the synthetic route. For example, Lercher and coworkers have studied methane oxidation in coppermetalated NU-1000 frameworks synthesized via gas-phase and solution-phase routes. 18,66 Gasphase metalation routes led to higher Cu loadings (10 wt%),66 whereas solution-phase metalation with copper(II) acetate generated lower Cu loadings (0.6-2.9 wt%).18 Both samples were pretreated with O₂ at 200 °C, exposed to CH₄, and then purged with H₂O/He to desorb the products of methane oxidation. While both frameworks exhibited similar methanol yields (11.1 mmol CH₃OH per mol Cu and 9.7 mmol CH₃OH per mol Cu for the gas-phase and solution-phase metalated materials, respectively), the solution-phase material shows markedly higher selectivity for methanol over other products (70% selectivity vs. 40-60%). For the gas-phase metalated material, the authors attributed the reactivity to predominantly tricopper clusters on the basis of extended X-ray absorption fine structure (EXAFS) data and density functional theory (DFT) calculations. 66 On the other hand, for the solution-phase metalated samples, reactivity was attributed to dicopper sites (Fig. 6b). 18 However, as both materials likely contain a complex distribution of isolated copper cations in addition to dimeric and oligomeric species, more rigorous spectroscopic investigation is needed to confirm the identity of the active sites.

In principle, it is possible to limit the formation of higher nuclearity clusters by carefully designing the binding pocket. For example, the framework MIL-125(Ti) is formed from cyclic $Ti_8(\mu_2-O)_8(\mu_2-OH)_4$ clusters, and has an overall formula of $Ti_8O_8(OH)_4(bdc)_6$ ($bdc^{2-}=1,4$ -benzenedicarboxylate).⁶⁸ The octameric titanium cluster creates a small cavity lined by four bridging hydroxides, with opposing hydroxides slightly less than 6 Å apart (**Fig. 6b**). Due to these steric constraints, Lin and coworkers showed that deprotonation of the bridging hydroxides and metalation with excess $Cu(CH_3CN)_4BF_4$ leads to the installation of just two copper centers per Ti_8 cluster (**Fig. 6b**).⁶⁹ A short Cu–Cu distance of 2.80 Å was observed by EXAFS. Mononuclear control samples could be made by using a subcess of the copper precursor. The binuclear system exhibited substantially higher activity for the aerobic epoxidation of olefins, with a TOF of 175 h^{-1} compared to 10 h^{-1} for the mononuclear control.

Another promising approach to control active site nuclearity is to use pre-formed bimetallic precursors, a strategy that was pioneered by the Lu group (**Fig. 6c**).^{70,71} This approach is particularly attractive for installing heterobimetallic sites. For example, cobalt-aluminum sites were installed in NU-1000 by treating it with a predefined molecular Co-Al complex, (py₃tren)-AlCoMe (py₃tren³⁻ = N,N,N-tris(2-(2pyridylamino)ethyl)amine). Further heating of the material at 300 °C under air resulted in the loss of the py₃tren ligand and the generation of a Co-Al diamond core.⁷⁰ Both the ligated and the heat-treated materials were competent catalysts for the oxidation of benzyl alcohol to benzaldehyde in the presence of *tert*-butyl hydroperoxide (TBHP), showing 7.5-fold greater activity per Co atom relative to the monometallic control framework. Similarly,

Ga-Rh–functionalized NU-1000 could be synthesized by soaking the framework in a solution of $(py_3tren)GaRhX$ (X = Me, OPh). Compared to molecular analogues and the Rh-only MOF, the Ga/Rh-functionalized catalyst showed much higher selectivity for *E*-alkenes in the semihydrogenation of diphenylacetylene.

2.2.2 Anchoring to Lewis acidic surface sites

In addition to Brønsted acidic hydroxyl sites, Lewis acidic surface sites can also be used as grafting points for post-synthetic metalation. For example, the nodes of MOF-808 contain monocarboxylates anchored to Lewis acidic Zr⁴⁺ metal centers (**Fig. 5**). These surface ligands can be exchanged with other anions, including ditopic ligands capable of binding additional metals.

Yaghi and coworkers leveraged the controlled stoichiometry of inward-facing capping ligands and the spatial constraints of the pores to install dicopper sites for the oxidation of methane to methanol (**Fig. 7**).¹⁷ Metal-binding sites were introduced into MOF-808 by exchanging the monoanionic capping ligands with different imidazole-containing carboxylic acids (e.g., L-histidine, 4-imidazoleacrylic acid, and 5-benzimidazolecarboxylic acid). A series of oxygen-bridged dicopper(II) sites were then installed by metalation with copper(I) iodide under air. To probe the reactivity of these copper-functionalized frameworks with methane, the frameworks were activated at 150 °C with flowing He, then treated sequentially with 3% N₂O/He, CH₄, and 3% steam/He. After this treatment, roughly 12.5–25 mmol MeOH was generated per mol Cu, depending on the ligand used.¹⁷ Given these yields, the speciation of copper is likely more complex than what is shown in **Fig. 7**, with a subpopulation of copper sites active for methane oxidation. While the authors use computational modeling to propose the active bridged copper dimers, additional spectroscopic evidence is needed to confirm the active site identity.

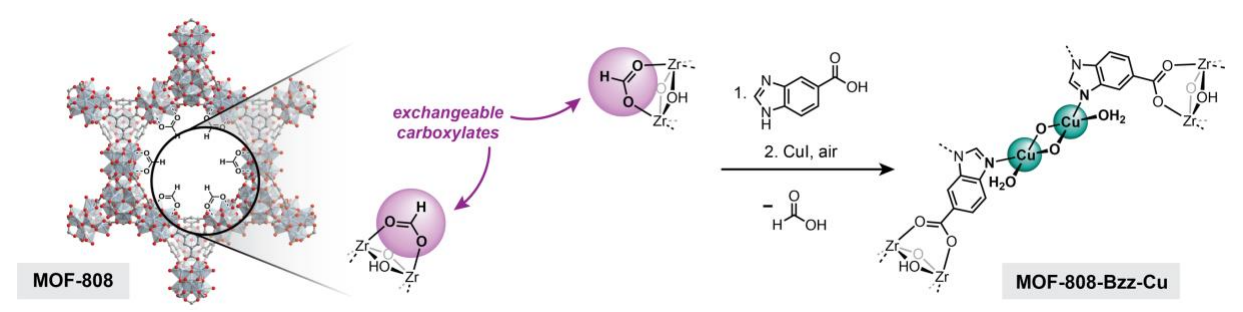


Fig. 7 | Grafting metal centers to Lewis-acidic surface sites in MOF-808. The exchange of anionic carboxylate ligands with imidazole-containing carboxylic acids is proposed to provide binding sites for copper(I) pairs. Figure based off reference 17.

2.2.3 Ion pairing

Ion-exchange methods can be used to install bimetallic sites in cationic or anionic metalorganic frameworks containing weakly bound counterions. In an elegant example of this strategy, Dincă, Román-Leshkov, and coworkers used post-synthetic anion exchange to electrostatically tether anionic [Co(CO)₄]⁻ complexes to the cationic trinuclear chromium(III) nodes of Cr-MIL-101 (**Fig. 8**).²² The strongly bound F⁻ anions in the as-synthesized framework were first exchanged

for more labile Cl⁻ anions, which were then exchanged for $[Co(CO)_4]^-$. This leads to heterobimetallic active sites where anionic metal carbonyl complexes are held in proximity to strongly Lewis acidic Cr(III) centers. Like the homogeneous [Lewis acid]⁺[Co(CO)_4]⁻ catalysts developed by Coates and coworkers,^{72,73} the Co(CO)₄-incorporated Cr-MIL-101 framework (abbreviated Co(CO)₄-Cr-MIL-101) is a highly active catalyst for the ring-expansion carbonylation of epoxides²² and β-Lactones.²³ We note that, relative to other tethering strategies, an advantage of the ion-pairing approach is that it offers much greater flexibility in the relative M– M distance and coordination sphere. For example, in Co(CO)₄-Cr-MIL-101, the Co(CO)₄-complex is free to adjust its primary coordination sphere and the relative Co–Cr distance.

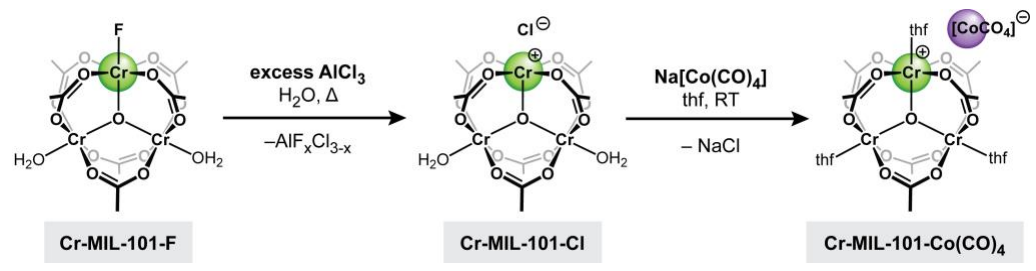


Fig. 8 | Overview of ion pairing strategy in Cr-MIL-101. Anchoring of $Co(CO)_4^-$ near the Lewis acidic Cr(III) sites is achieved through stepwise ion exchange to yield bimetallic Cr/Co sites for ring-expansion carbonylation of epoxides and β-Lactones. For clarity, ligands have been truncated at the terminal carboxylate unit. Figure based off reference 22.

2.3 Grafting to ligand struts

In addition to grafting metal cations to the framework nodes, it is also possible to install metal chelating sites to the framework struts. One advantage of this approach is the diversity of ligand environments that can be obtained (**Fig. 9**). Binding sites can be pre-integrated into the ligand strut and installed during framework formation. Bipyridine, ^{74–76} salen, ⁷⁷ porphyrin, ^{78–80} and dipyrazole groups have been incorporated using this route (**Fig. 9a**). Chelating sites can also be installed after MOF synthesis through post-synthetic ligand exchange or covalent modification strategies. Iminopyridine, ⁸² salicylidene, ⁸³ aminopyridineimine, ⁸⁴ and bis(2-pyridylmethyl)amine groups, among others, have been introduced in this manner (**Fig. 9b**). These different strategies have been comprehensively summarized by Moon and coworkers in a recent review. ⁸⁶

While the metalation of ligand struts was initially developed for mononuclear metal complexes, researchers have recently extended these methods to bimetallic active sites. As with grafting to the metal nodes, the dominant challenge is controlling active site nuclearity. At low surface coverages, mononuclear sites dominate, while at high coverages larger clusters can form. Several strategies to overcome this challenge have been reported, including the use of pre-formed clusters (Section 2.3.1) and exogenous bridging ligands to dimerize metals bound to neighboring struts (Section 2.3.2). In addition, templating approaches have been developed to selectively functionalize neighboring ligands (Section 2.3.3).

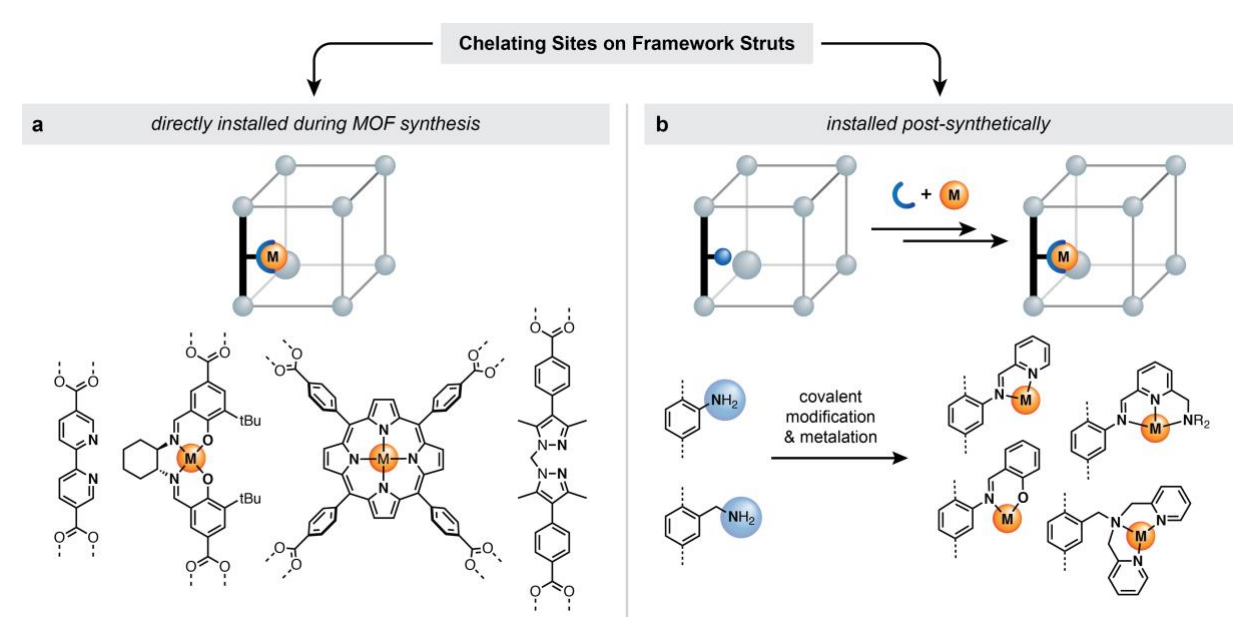


Fig. 9 | Overview of strategies to install metal-binding sites on ligand struts. Chelating sites can be installed either a) during synthesis, or b) after synthesis via post-synthetic modification strategies.

2.3.1 Anchoring pre-formed clusters

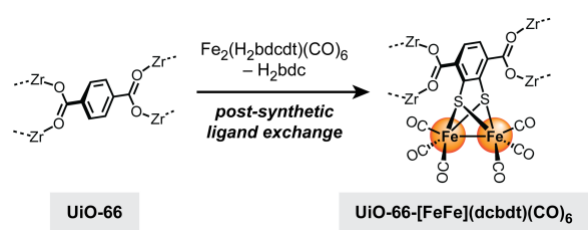


Fig. 10 | Overview of post-synthetic ligand exchange to install pre-formed dithiolate diiron clusters in UiO-66 for photocatalytic proton reduction. Figure based off reference 19.

Using a post-synthetic ligand exchange strategy, Cohen, Ott, and coworkers were able to attach dithiolate-bound diiron clusters to the struts of UiO-66 (**Fig. 10**). ¹⁹ Up to 14% of the original 1,4-benzenedicarboxylate ligands could be exchanged for a diiron-functionalized strut, $[Fe_2(dcbdt)(CO)_6]^{2-}$ ($dcbdt^{2-} = 1,4$ -dicarboxylbenzene-2,3-dithiolate). One advantage of using pre-formed clusters is their structural fidelity. Extended X-ray absorption

fine structure (EXAFS) spectroscopy confirmed that the local coordination environment around the iron centers in UiO-66-[FeFe](dcbdt)(CO)₆ is identical to molecular analogues, with a short Fe–Fe distance of \sim 2.4 Å. The MOF-supported diiron system, which closely resembles the active site of [FeFe] hydrogenases, catalyzes the photocatalytic reduction of protons into H₂ in the presence of [Ru(bpy)₃]²⁺ as the photosensitizer and ascorbate as the electron donor. Relative to a molecular analogue, the MOF-supported dimer showed both higher initial rates and greater overall production of H₂.

2.3.2 Anchoring to neighboring ligand struts

Metal-organic frameworks constructed from 1D metal-ligand chains (also called "rod-shaped" secondary building units) often display one-dimensional pore channels that are densely lined with bridging ligands. ^{87,88} In these frameworks, anchoring metals to neighboring struts is an

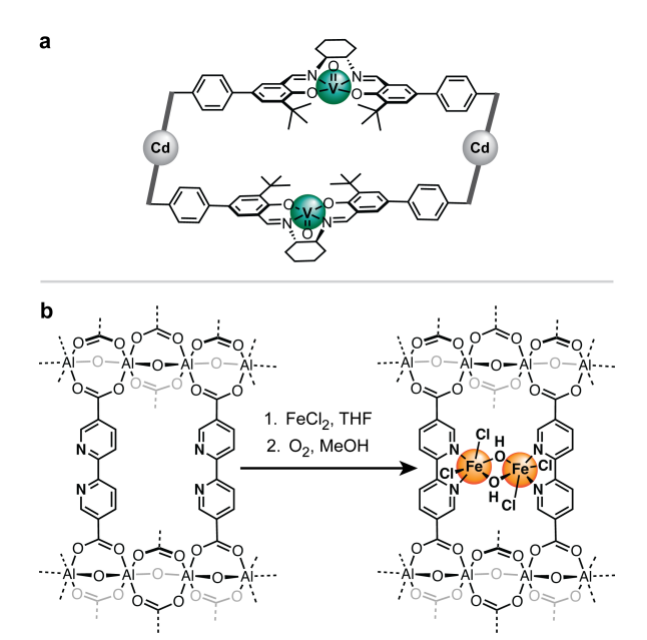


Fig. 11 | Neighboring ligand struts can be used to install (a) bimetallic vanadyl sites for asymmetric aldehyde cyanation and (b) Fe(III) dimers for benzylic C–H oxidation and alkene epoxidation. Figures based off references 89 and 90.

appealing way to design bimetallic sites due to the short distance between adjacent ligands (\sim 6–10 Å).

A nice example of this strategy was reported by Cui and coworkers in 2016, who synthesized a Cd-based framework with 1D channels lined with chiral vanadium-salen units (**Fig. 11a**). 89 The authors showed that the neighboring vanadyl sites, which are roughly 8 Å apart, work together to activate and preorient the substrates for the asymmetric cyanation of aldehydes. To confirm the bimetallic nature of the mechanism, an isostructural framework with alternating vanadium and copper sites was used, which showed both lower conversion (50% vs. 98%) and lower enantioselectivity (75% ee vs. 86% ee) than the all-vanadium framework.

In 2023, Lin and coworkers used this

strategy to generate bimetallic sites in a bipyridyl-decorated aluminum framework, MOF-253 (also known as Al(OH)bpydc, bpydc $^{2-}$ = 2,2'-bipyridine-5,5'-dicarboxylate). The framework, which is isostructural with MIL-53, contains rhombic, one-dimensional channels lined with 2,2'-bipyridine-functionalized struts spaced roughly 6.6 Å apart. Metalation of the bipyridine units with FeCl₂ followed by bubbling O₂ in MeOH resulted in the formation of dihydroxo-bridged Fe(III) dimers (**Fig. 11b**). The Fe₂(μ -OH)₂ dimers were characterized by EXAFS, which showed a strong Fe–Fe scattering feature consistent with the expected ~3 Å distance between Fe sites. The diiron MOF was a competent catalyst for both benzylic C–H oxidation and alkene epoxidation reactions using O₂ as the oxidant and pivaldehyde as the sacrificial reductant. A mononuclear control framework was synthesized where only ~11% of the ligands are functionalized with bipyridine units. The bimetallic framework showed a 27-fold increase in activity compared to the mononuclear control, highlighting the impact of the bimetallic sites.

2.3.3 Templating approaches

As described in <u>Section 2.3.2</u>, neighboring ligand struts can support the formation of well-defined bimetallic sites with the addition of exogenous bridging ligands such as hydroxide (**Fig. 11**). However, this strategy is less effective at lower metal loadings, as it is difficult to control the relative distribution of partially metalated ligand struts. At low loadings, isolated mononuclear metal sites are predominantly formed. This can be limiting, as lower metal loadings may be desired to reduce pore clogging or prevent cross-reactivity between neighboring active sites.

To address this challenge, we recently reported a strategy to introduce closely spaced pairs of functional groups within MOF pores, irrespective of functional group loading. We first showed that thermolabile tertiary ester-based crosslinkers can be used to template pairs of carboxylic acids \sim 7 Å apart down the pore channels of Mg2dotpdc (dotpdc⁴⁻ = 4,4"-dioxido-[1,1':4',1"-terphenyl]-3,3"-dicarboxylate), a mesoporous framework with one-dimensional hexagonal channels. We later developed tertiary carbamate-based crosslinkers that, upon thermolysis, reveal pairs of templated amines (**Fig. 12a**). These amine pairs could be post-synthetically elaborated into iminopyridine and bis(2-pyridylmethyl)amine chelating sites (**Fig. 12b**) and metalated with a variety of first-row transition metals (M = Mn(II), Fe(II), Co(II), Ni(II), Cu(I), and Cu(II)).

Relative to the other synthetic approaches described here, templating strategies require much larger upfront synthetic investment, as a suitable labile crosslinker must first be designed and incorporated into the desired framework. However, once the templated functional groups are installed, there is the potential for rapid catalyst derivatization via well-established post-synthetic modification reactions. Indeed, the main advantage of molecular templating is the structural versatility. In principle, it should be possible to independently control the pore architecture, metal identity, local ligand environment, and metal—metal distance of the templated bimetallic sites.

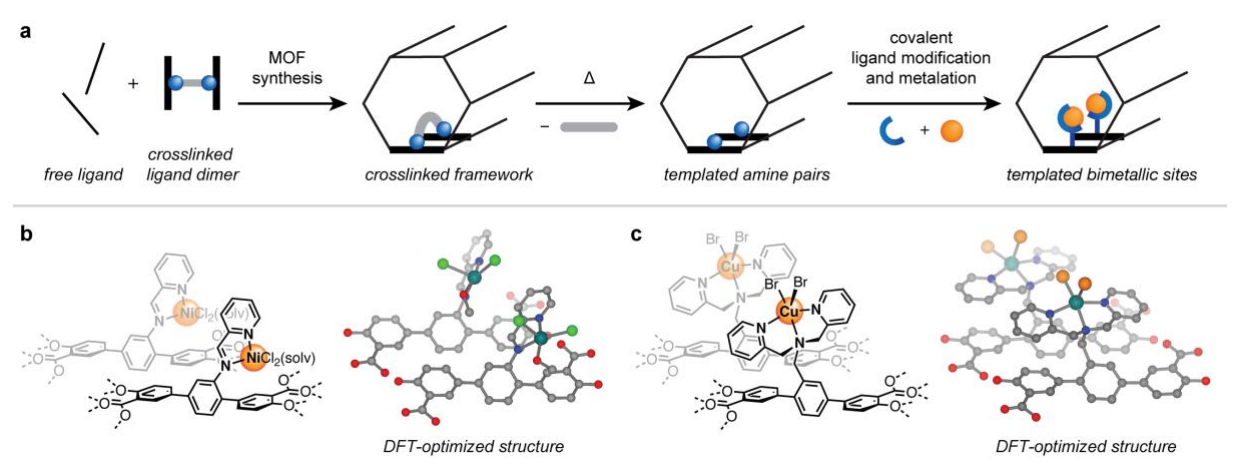


Fig. 12 | a) Thermolabile crosslinkers can be used to template amine pairs, which can be elaborated into bimetallic sites with tunable ligand environments, such as b) iminopyridine and c) bis(2-pyridylmethyl)amine. Figure adapted from reference 85.

2.4 Other strategies

A combination of grafting approaches can also be used to generate bimetallic sites, such as attaching one metal to the framework nodes and the other to the struts. For example, Lin and coworkers took advantage of distinct metal node and ligand strut chemistry to functionalize hafnium-based metal—organic sheets with both Ru-based photosensitizers and Re or Mn-based cocatalysts (**Fig. 13**).⁹² The Ru-based photosensitizer was bound to bipyridine-functionalized struts and installed directly during framework synthesis. The Re or Mn-based cocatalyst was post-synthetically grafted to the metal nodes by exchanging surface-bound trifluoroacetate groups with carboxylate-functionalized bipyridine ligands and metalating with either Re(CO)₅Cl and Mn(CO)₅Br. Both Ru/Re and Ru/Mn systems showed good activity for the photoreduction of CO₂

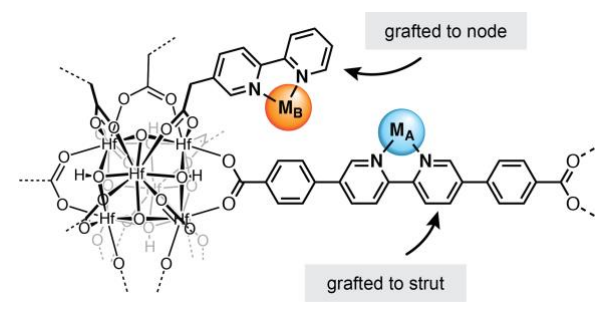


Fig. 13 | Multiple grafting strategies can be used in tandem. For example, Ru-based photosensitizers at the ligand struts can work cooperatively with Re or Mn cocatalysts post-synthetically grafted to the Hf cluster through carboxylate exchange. Figure based off reference 92.

to CO in the presence of sacrificial electron donors, with turnover numbers of up to 3849 and 1367 after 25 h, respectively. Greater than 70-fold increase in catalytic activity was observed in the MOF systems relative to homogeneous controls, which the authors attributed to the proximity of the Ru photosensitizer to the catalytic Re/Mn centers.

3 Critical assessment and future outlook

The synthesis of binuclear metal active sites in metal-organic frameworks has seen significant progress over the last decade.

While barriers to controlling active site nuclearity remain, promising solutions are already emerging, including the use of pre-formed clusters, 19,58,70,71 sterically constrained binding pockets, 69 and templating approaches. 85,91 We conclude this perspective by shifting our focus away from synthetic strategies and towards the future potential of these materials as heterogeneous catalysts. Below, we highlight unique opportunities for MOF-supported bimetallic catalysis as well as outstanding challenges.

Rigorous characterization of active site structure: The conclusive spectroscopic identification of binuclear sites remains an open challenge in MOF catalysis and is critical for advancing the field. In many of the examples highlighted in this perspective, a complex distribution of metal species is both observed spectroscopically as well as inferred by the relatively low yields of product per metal in stoichiometric reactions. While initial reports have placed greater emphasis on synthesis and reactivity, going forward more detailed spectroscopic investigations are needed to understand the initial metal speciation, identify which species are catalytically relevant, and determine how these structural distributions change over time.

Balancing active site rigidity vs. flexibility: In certain cases, active site rigidity is beneficial. Geometric constraints enforced by rigid protein superstructures and zeolite lattices can lead metal sites to adopt unusual coordination environments, generating highly reactive "entatic" states. 10,93 At the same time, greater active site flexibility can also be advantageous, as different intermediates may be stabilized by subtly different active site conformations. One advantage of metal—organic frameworks is the ability to accommodate structures at both extremes as well as the many gradations in between. For example, the rigid multinuclear metal nodes discussed in Section 2.1 greatly constrain the possible M–M distances and coordination environments that can be accessed during catalysis, while the electrostatically tethered ion pairs discussed in Section 2.2.3 offers much greater flexibility. Going forward, a challenge in catalyst design will be navigating the wealth of choices and selecting the appropriate balance of flexibility and rigidity for a given catalytic application.

Leveraging pore environment effects: Many of the reports highlighted in this perspective focus on tuning the primary coordination sphere of the two metal sites. In contrast, the interplay between the binuclear active site and its surrounding pore environment remains understudied. The enzymelike ability of metal—organic frameworks to control and confine the surrounding three-dimensional microenvironment is a distinct yet underutilized advantage of MOF catalysts. ^{94–96} We note that this is a challenge and opportunity for all MOF catalysis, beyond the binuclear active sites focused on here.

Higher throughput catalyst synthesis and screening: Studies in this field generally report a single bimetallic active site design for a single target reaction. To accelerate catalyst discovery, greater throughput in catalyst synthesis and screening is needed. If the synthetic advances described in this perspective have uncovered a treasure chest of bimetallic MOF systems, then high throughput experimentation may be the key to unlock their untapped potential as catalysts.

Assessing active site stability: While significant strides in metal—organic framework stability have been made, ^{97,98} active sites can be degraded even if the surrounding pore structure remains intact. For example, in the absence of strongly chelating groups, surface-grafted systems may be susceptible to metal leaching. Initially well-defined systems may lose structural fidelity if metal cations become mobile under reaction conditions. In addition to identifying active site degradation mechanisms, strategies to mitigate degradation and regenerate spent catalysts are needed.

In conclusion, metal—organic frameworks provide an exciting opportunity to re-examine bioinspired and organometallic binuclear active sites in a heterogeneous context. It is possible that greater catalytic activity, selectivity, and/or stability can be realized due to properties unique to porous scaffolds, including site isolation, entatic states, and microenvironment effects. Going forward, coupling existing synthetic routes with greater throughput catalyst screening and more rigorous characterization may reveal new reactivity not yet observed in other heterogeneous or homogeneous platforms.

4 Author Information

Corresponding author

Dianne Xiao – Department of Chemistry, University of Washington, Seattle, Washington 98195, United States; Email: djxiao@uw.edu

Authors

Jackson Geary – Department of Chemistry, University of Washington, Seattle, Washington 98195, United States

Author Contributions

The manuscript was written through contributions of all authors. All authors have given approval to the final version of the manuscript.

Notes

The authors declare no competing financial interest.

Biographies

Jackson Geary received his B.S. in Chemistry from the University of Utah in 2018. He is currently pursuing his Ph.D. in the lab of Dr. Dianne Xiao at the University of Washington as a National Science Foundation (NSF) graduate research fellow. His research is focused on the development of new synthetic strategies to install precise multicomponent active sites inside metal—organic framework pores, with an emphasis on the installation of templated bimetallic sites.

Dianne J. Xiao is an Assistant Professor in the Department of Chemistry at the University of Washington. She received her A.B. from Harvard College in 2011 and her Ph.D. from the University of California, Berkeley in 2016. She completed postdoctoral studies at Stanford University before beginning her independent career in 2019. Her synthesis-driven research program aims to endow porous materials with the enhanced reactivity and physical properties needed to meet rising global challenges in clean energy and sustainability.

5 Acknowledgements

This material is based upon work supported by the National Science Foundation under Grant No. 2142798 and the David and Lucile Packard Foundation. J.G. is supported by an NSF graduate research fellowship.

6 References

- (1) Lubitz, W.; Ogata, H.; Rüdiger, O.; Reijerse, E. Hydrogenases. *Chem. Rev.* **2014**, *114* (8), 4081–4148. https://doi.org/10.1021/cr4005814.
- (2) Elwell, C. E.; Gagnon, N. L.; Neisen, B. D.; Dhar, D.; Spaeth, A. D.; Yee, G. M.; Tolman, W. B. Copper–Oxygen Complexes Revisited: Structures, Spectroscopy, and Reactivity. *Chem. Rev.* **2017**, *117* (3), 2059–2107. https://doi.org/10.1021/acs.chemrev.6b00636.
- (3) Jasniewski, A. J.; Que, L. Dioxygen Activation by Nonheme Diiron Enzymes: Diverse Dioxygen Adducts, High-Valent Intermediates, and Related Model Complexes. *Chem. Rev.* **2018**, *118* (5), 2554–2592. https://doi.org/10.1021/acs.chemrev.7b00457.
- (4) Snyder, B. E. R.; Bols, M. L.; Schoonheydt, R. A.; Sels, B. F.; Solomon, E. I. Iron and Copper Active Sites in Zeolites and Their Correlation to Metalloenzymes. *Chem. Rev.* **2018**, *118* (5), 2718–2768. https://doi.org/10.1021/acs.chemrev.7b00344.
- (5) Wilcox, D. E. Binuclear Metallohydrolases. *Chem. Rev.* **1996**, *96* (7), 2435–2458. https://doi.org/10.1021/cr950043b.
- (6) Mitić, N.; Smith, S. J.; Neves, A.; Guddat, L. W.; Gahan, L. R.; Schenk, G. The Catalytic Mechanisms of Binuclear Metallohydrolases. *Chem. Rev.* **2006**, *106* (8), 3338–3363. https://doi.org/10.1021/cr050318f.

- (7) Delferro, M.; Marks, T. J. Multinuclear Olefin Polymerization Catalysts. *Chem. Rev.* **2011**, *111* (3), 2450–2485. https://doi.org/10.1021/cr1003634.
- (8) Cooper, B. G.; Napoline, J. W.; Thomas, C. M. Catalytic Applications of Early/Late Heterobimetallic Complexes. *Catalysis Reviews* **2012**, *54* (1), 1–40. https://doi.org/10.1080/01614940.2012.619931.
- (9) Cammarota, R. C.; Clouston, L. J.; Lu, C. C. Leveraging Molecular Metal–Support Interactions for H2 and N2 Activation. *Coordination Chemistry Reviews* **2017**, *334*, 100–111. https://doi.org/10.1016/j.ccr.2016.06.014.
- (10) Rhoda, H. M.; Heyer, A. J.; Snyder, B. E. R.; Plessers, D.; Bols, M. L.; Schoonheydt, R. A.; Sels, B. F.; Solomon, E. I. Second-Sphere Lattice Effects in Copper and Iron Zeolite Catalysis. *Chem. Rev.* **2022**, *122* (14), 12207–12243. https://doi.org/10.1021/acs.chemrev.1c00915.
- (11) Li, X.; Liu, L.; Ren, X.; Gao, J.; Huang, Y.; Liu, B. Microenvironment Modulation of Single-Atom Catalysts and Their Roles in Electrochemical Energy Conversion. *Sci. Adv.* **2020**, *6* (39), eabb6833. https://doi.org/10.1126/sciadv.abb6833.
- (12) Liu, J.; Goetjen, T. A.; Wang, Q.; Knapp, J. G.; Wasson, M. C.; Yang, Y.; Syed, Z. H.; Delferro, M.; Notestein, J. M.; Farha, O. K.; Hupp, J. T. MOF-Enabled Confinement and Related Effects for Chemical Catalyst Presentation and Utilization. *Chem. Soc. Rev.* **2022**, *51* (3), 1045–1097. https://doi.org/10.1039/D1CS00968K.
- (13) Liu, L.; Corma, A. Bimetallic Sites for Catalysis: From Binuclear Metal Sites to Bimetallic Nanoclusters and Nanoparticles. *Chem. Rev.* **2023**, *123* (8), 4855–4933. https://doi.org/10.1021/acs.chemrev.2c00733.
- (14) Kulkarni, A.; Lobo-Lapidus, R. J.; Gates, B. C. Metal Clusters on Supports: Synthesis, Structure, Reactivity, and Catalytic Properties. *Chem. Commun.* **2010**, *46* (33), 5997. https://doi.org/10.1039/c002707n.
- (15) Wang, J.; Li, G.; Li, Z.; Tang, C.; Feng, Z.; An, H.; Liu, H.; Liu, T.; Li, C. A Highly Selective and Stable ZnO-ZrO2 Solid Solution Catalyst for CO2 Hydrogenation to Methanol. *Science Advances* **2017**, *3* (10), e1701290. https://doi.org/10.1126/sciadv.1701290.
- (16) Osadchii, D. Y.; Olivos-Suarez, A. I.; Szécsényi, Á.; Li, G.; Nasalevich, M. A.; Dugulan, I. A.; Crespo, P. S.; Hensen, E. J. M.; Veber, S. L.; Fedin, M. V.; Sankar, G.; Pidko, E. A.; Gascon, J. Isolated Fe Sites in Metal Organic Frameworks Catalyze the Direct Conversion of Methane to Methanol. *ACS Catalysis* **2018**, *8* (6), 5542–5548. https://doi.org/10.1021/ACSCATAL.8B00505.
- (17) Baek, J.; Rungtaweevoranit, B.; Pei, X.; Park, M.; Fakra, S. C.; Liu, Y.-S.; Matheu, R.; Alshmimri, S. A.; Alshehri, S.; Trickett, C. A.; Somorjai, G. A.; Yaghi, O. M. Bioinspired Metal–Organic Framework Catalysts for Selective Methane Oxidation to Methanol. *J. Am. Chem. Soc.* **2018**, *140* (51), 18208–18216. https://doi.org/10.1021/jacs.8b11525.
- (18) Zheng, J.; Ye, J.; Ortuño, M. A.; Fulton, J. L.; Gutiérrez, O. Y.; Camaioni, D. M.; Motkuri, R. K.; Li, Z.; Webber, T. E.; Mehdi, B. L.; Browning, N. D.; Penn, R. L.; Farha, O. K.; Hupp, J. T.; Truhlar, D. G.; Cramer, C. J.; Lercher, J. A. Selective Methane Oxidation to Methanol on Cu-Oxo Dimers Stabilized by Zirconia Nodes of an NU-1000 Metal–Organic Framework. *J. Am. Chem. Soc.* **2019**, *141* (23), 9292–9304. https://doi.org/10.1021/jacs.9b02902.

- (19) Pullen, S.; Fei, H.; Orthaber, A.; Cohen, S. M.; Ott, S. Enhanced Photochemical Hydrogen Production by a Molecular Diiron Catalyst Incorporated into a Metal–Organic Framework. *J. Am. Chem. Soc.* **2013**, *135* (45), 16997–17003. https://doi.org/10.1021/ja407176p.
- (20) Castner, A. T.; Johnson, B. A.; Cohen, S. M.; Ott, S. Mimicking the Electron Transport Chain and Active Site of [FeFe] Hydrogenases in One Metal—Organic Framework: Factors That Influence Charge Transport. *J. Am. Chem. Soc.* **2021**, *143* (21), 7991–7999. https://doi.org/10.1021/jacs.1c01361.
- (21) Zhang, J.; An, B.; Li, Z.; Cao, Y.; Dai, Y.; Wang, W.; Zeng, L.; Lin, W.; Wang, C. Neighboring Zn–Zr Sites in a Metal–Organic Framework for CO₂ Hydrogenation. *J. Am. Chem. Soc.* **2021**, *143* (23), 8829–8837. https://doi.org/10.1021/jacs.1c03283.
- (22) Park, H. D.; Dincă, M.; Román-Leshkov, Y. Heterogeneous Epoxide Carbonylation by Cooperative Ion-Pair Catalysis in Co(CO) 4 Incorporated Cr-MIL-101. *ACS Cent. Sci.* **2017**, *3* (5), 444–448. https://doi.org/10.1021/acscentsci.7b00075.
- (23) Park, H. D.; Dincă, M.; Román-Leshkov, Y. Continuous-Flow Production of Succinic Anhydrides via Catalytic β-Lactone Carbonylation by Co(CO) 4 ⊂Cr-MIL-101. *J. Am. Chem. Soc.* **2018**, *140* (34), 10669–10672. https://doi.org/10.1021/jacs.8b05948.
- (24) Gascon, J.; Corma, A.; Kapteijn, F.; Llabrés i Xamena, F. X. Metal Organic Framework Catalysis: *Quo Vadis*? *ACS Catal.* **2014**, *4* (2), 361–378. https://doi.org/10.1021/cs400959k.
- (25) Song, Y.; Feng, X.; Lin, W. Metal-Organic Frameworks for Catalytic Applications. In *Comprehensive Coordination Chemistry III*; Elsevier, 2021; pp 228–259. https://doi.org/10.1016/B978-0-08-102688-5.00025-8.
- (26) Zheng, W.; Lee, L. Y. S. Metal–Organic Frameworks for Electrocatalysis: Catalyst or Precatalyst? *ACS Energy Lett.* **2021**, *6* (8), 2838–2843. https://doi.org/10.1021/acsenergylett.1c01350.
- (27) Al-Rowaili, F. N.; Jamal, A.; Ba Shammakh, M. S.; Rana, A. A Review on Recent Advances for Electrochemical Reduction of Carbon Dioxide to Methanol Using Metal—Organic Framework (MOF) and Non-MOF Catalysts: Challenges and Future Prospects. *ACS Sustainable Chem. Eng.* **2018**, *6* (12), 15895–15914. https://doi.org/10.1021/acssuschemeng.8b03843.
- (28) Li, C.; Zhang, H.; Liu, M.; Lang, F.-F.; Pang, J.; Bu, X.-H. Recent Progress in Metal—Organic Frameworks (MOFs) for Electrocatalysis. *Ind. Chem. Mater.* **2023**, *1* (1), 9–38. https://doi.org/10.1039/D2IM00063F.
- (29) Zhang, T.; Lin, W. Metal–Organic Frameworks for Artificial Photosynthesis and Photocatalysis. *Chem. Soc. Rev.* **2014**, *43* (16), 5982–5993. https://doi.org/10.1039/C4CS00103F.
- (30) Wang, J.-L.; Wang, C.; Lin, W. Metal–Organic Frameworks for Light Harvesting and Photocatalysis. *ACS Catal.* **2012**, *2* (12), 2630–2640. https://doi.org/10.1021/cs3005874.
- (31) Whelan, É.; Steuber, F. W.; Gunnlaugsson, T.; Schmitt, W. Tuning Photoactive Metal–Organic Frameworks for Luminescence and Photocatalytic Applications. *Coordination Chemistry Reviews* **2021**, *437*, 213757. https://doi.org/10.1016/j.ccr.2020.213757.
- (32) Liu, M.; Xing, Z.; Li, Z.; Zhou, W. Recent Advances in Core–Shell Metal Organic Frame-Based Photocatalysts for Solar Energy Conversion. *Coordination Chemistry Reviews* **2021**, 446, 214123. https://doi.org/10.1016/j.ccr.2021.214123.

- (33) Dai, S.; Tissot, A.; Serre, C. Recent Progresses in Metal–Organic Frameworks Based Core–Shell Composites. *Advanced Energy Materials* **2022**, *12* (4), 2100061. https://doi.org/10.1002/aenm.202100061.
- (34) Hong, D. H.; Shim, H. S.; Ha, J.; Moon, H. R. MOF-on-MOF Architectures: Applications in Separation, Catalysis, and Sensing. *Bulletin of the Korean Chemical Society* **2021**, *42* (7), 956–969. https://doi.org/10.1002/bkcs.12335.
- (35) Zhao, Z.; Ding, J.; Zhu, R.; Pang, H. The Synthesis and Electrochemical Applications of Core–Shell MOFs and Their Derivatives. *J. Mater. Chem. A* **2019**, *7* (26), 15519–15540. https://doi.org/10.1039/C9TA03833G.
- (36) Chen, L.; Wang, H.-F.; Li, C.; Xu, Q. Bimetallic Metal–Organic Frameworks and Their Derivatives. *Chem. Sci.* **2020**, *11* (21), 5369–5403. https://doi.org/10.1039/D0SC01432J.
- (37) Konnerth, H.; Matsagar, B. M.; Chen, S. S.; Prechtl, M. H. G.; Shieh, F.-K.; Wu, K. C.-W. Metal-Organic Framework (MOF)-Derived Catalysts for Fine Chemical Production. *Coordination Chemistry Reviews* **2020**, *416*, 213319. https://doi.org/10.1016/j.ccr.2020.213319.
- (38) Hao, M.; Qiu, M.; Yang, H.; Hu, B.; Wang, X. Recent Advances on Preparation and Environmental Applications of MOF-Derived Carbons in Catalysis. *Science of The Total Environment* **2021**, *760*, 143333. https://doi.org/10.1016/j.scitotenv.2020.143333.
- (39) Liu, D.; Gu, W.; Zhou, L.; Wang, L.; Zhang, J.; Liu, Y.; Lei, J. Recent Advances in MOF-Derived Carbon-Based Nanomaterials for Environmental Applications in Adsorption and Catalytic Degradation. *Chemical Engineering Journal* **2022**, *427*, 131503. https://doi.org/10.1016/j.cej.2021.131503.
- (40) Mukoyoshi, M.; Kitagawa, H. Nanoparticle/Metal—Organic Framework Hybrid Catalysts: Elucidating the Role of the MOF. *Chemical Communications* **2022**, *58* (77), 10757–10767. https://doi.org/10.1039/D2CC03233C.
- (41) Xiang, W.; Zhang, Y.; Lin, H.; Liu, C. Nanoparticle/Metal—Organic Framework Composites for Catalytic Applications: Current Status and Perspective. *Molecules* **2017**, *22* (12), 2103. https://doi.org/10.3390/molecules22122103.
- (42) McDonald, T. M.; Mason, J. A.; Kong, X.; Bloch, E. D.; Gygi, D.; Dani, A.; Crocellà, V.; Giordanino, F.; Odoh, S. O.; Drisdell, W. S.; Vlaisavljevich, B.; Dzubak, A. L.; Poloni, R.; Schnell, S. K.; Planas, N.; Lee, K.; Pascal, T.; Wan, L. F.; Prendergast, D.; Neaton, J. B.; Smit, B.; Kortright, J. B.; Gagliardi, L.; Bordiga, S.; Reimer, J. A.; Long, J. R. Cooperative Insertion of CO2 in Diamine-Appended Metal-Organic Frameworks. *Nature* 2015, 519 (7543), 303–308. https://doi.org/10.1038/nature14327.
- (43) Reed, D. A.; Keitz, B. K.; Oktawiec, J.; Mason, J. A.; Runčevski, T.; Xiao, D. J.; Darago, L. E.; Crocellà, V.; Bordiga, S.; Long, J. R. A Spin Transition Mechanism for Cooperative Adsorption in Metal–Organic Frameworks. *Nature* **2017**, *550* (7674), 96–100. https://doi.org/10.1038/nature23674.
- (44) Bien, C. E.; Chen, K. K.; Chien, S.-C.; Reiner, B. R.; Lin, L.-C.; Wade, C. R.; Ho, W. S. W. Bioinspired Metal–Organic Framework for Trace CO2 Capture. *J. Am. Chem. Soc.* **2018**, *140* (40), 12662–12666. https://doi.org/10.1021/jacs.8b06109.
- (45) Wang, C.-H.; Das, A.; Gao, W.-Y.; Powers, D. C. Probing Substrate Diffusion in Interstitial MOF Chemistry with Kinetic Isotope Effects. *Angew. Chem. Int. Ed.* **2018**, *57* (14), 3676–3681. https://doi.org/10.1002/anie.201713244.

- (46) Wang, C.-H.; Gao, W.-Y.; Powers, D. C. Measuring and Modulating Substrate Confinement during Nitrogen-Atom Transfer in a Ru 2 -Based Metal-Organic Framework. *J. Am. Chem. Soc.* **2019**, *141* (49), 19203–19207. https://doi.org/10.1021/jacs.9b09620.
- (47) Liu, Q.; Song, Y.; Ma, Y.; Zhou, Y.; Cong, H.; Wang, C.; Wu, J.; Hu, G.; O'Keeffe, M.; Deng, H. Mesoporous Cages in Chemically Robust MOFs Created by a Large Number of Vertices with Reduced Connectivity. *J. Am. Chem. Soc.* **2019**, *141* (1), 488–496. https://doi.org/10.1021/jacs.8b11230.
- (48) Li, M.; Chen, J.; Wu, W.; Fang, Y.; Dong, S. Oxidase-like MOF-818 Nanozyme with High Specificity for Catalysis of Catechol Oxidation. *J. Am. Chem. Soc.* **2020**, *142* (36), 15569–15574. https://doi.org/10.1021/jacs.0c07273.
- (49) Hall, J. N.; Bollini, P. Low-Temperature, Ambient Pressure Oxidation of Methane to Methanol Over Every Tri-Iron Node in a Metal–Organic Framework Material. *Chemistry A European Journal* **2020**, *26* (70), 16639–16643. https://doi.org/10.1002/chem.202003894.
- (50) Simons, M. C.; Prinslow, S. D.; Babucci, M.; Hoffman, A. S.; Hong, J.; Vitillo, J. G.; Bare, S. R.; Gates, B. C.; Lu, C. C.; Gagliardi, L.; Bhan, A. Beyond Radical Rebound: Methane Oxidation to Methanol Catalyzed by Iron Species in Metal–Organic Framework Nodes. *J. Am. Chem. Soc.* **2021**, *143* (31), 12165–12174. https://doi.org/10.1021/jacs.1c04766.
- (51) Dincă, M.; Dailly, A.; Liu, Y.; Brown, C. M.; Neumann, Dan. A.; Long, J. R. Hydrogen Storage in a Microporous Metal—Organic Framework with Exposed Mn ²⁺ Coordination Sites. *J. Am. Chem. Soc.* **2006**, *128* (51), 16876–16883. https://doi.org/10.1021/ja0656853.
- (52) He, X.; Iliescu, A.; Yang, T.; Arguilla, M. Q.; Chen, T.; Kulik, H. J.; Dincă, M. Reversible O–O Bond Scission and O 2 Evolution at MOF-Supported Tetramanganese Clusters. *J. Am. Chem. Soc.* **2023**, *145* (30), 16872–16878. https://doi.org/10.1021/jacs.3c05374.
- (53) Cai, Z.; Tao, W.; Moore, C. E.; Zhang, S.; Wade, C. R. Direct NO Reduction by a Biomimetic Iron(II) Pyrazolate MOF. *Angew Chem Int Ed* **2021**, *60* (39), 21221–21225. https://doi.org/10.1002/anie.202108095.
- (54) Serre, C.; Millange, F.; Thouvenot, C.; Noguès, M.; Marsolier, G.; Louër, D.; Férey, G. Very Large Breathing Effect in the First Nanoporous Chromium(III)-Based Solids: MIL-53 or CrIII(OH)·{O2C-C6H4-CO2}·{HO2C-C6H4-CO2H}x·H2Oy. *J. Am. Chem. Soc.* **2002**, *124* (45), 13519–13526. https://doi.org/10.1021/ja0276974.
- (55) Barthelet, K.; Marrot, J.; Riou, D.; Férey, G. A Breathing Hybrid Organic–Inorganic Solid with Very Large Pores and High Magnetic Characteristics. *Angewandte Chemie International Edition* **2002**, *41* (2), 281–284. https://doi.org/10.1002/1521-3773(20020118)41:2<281::AID-ANIE281>3.0.CO;2-Y.
- (56) Loiseau, T.; Serre, C.; Huguenard, C.; Fink, G.; Taulelle, F.; Henry, M.; Bataille, T.; Férey, G. A Rationale for the Large Breathing of the Porous Aluminum Terephthalate (MIL-53) Upon Hydration. *Chemistry A European Journal* **2004**, *10* (6), 1373–1382. https://doi.org/10.1002/chem.200305413.
- (57) Whitfield, T. R.; Wang, X.; Liu, L.; Jacobson, A. J. Metal-Organic Frameworks Based on Iron Oxide Octahedral Chains Connected by Benzenedicarboxylate Dianions. *Solid State Sciences* **2005**, *7* (9), 1096–1103. https://doi.org/10.1016/j.solidstatesciences.2005.03.007.
- (58) López-García, C.; Canossa, S.; Hadermann, J.; Gorni, G.; Oropeza, F. E.; de la Peña O'Shea, V. A.; Iglesias, M.; Angeles Monge, M.; Gutiérrez-Puebla, E.; Gándara, F. Heterometallic Molecular Complexes Act as Messenger Building Units to Encode Desired

- Metal-Atom Combinations to Multivariate Metal-Organic Frameworks. *J. Am. Chem. Soc.* **2022**. https://doi.org/10.1021/jacs.2c06142.
- (59) Yang, D.; Babucci, M.; Casey, W. H.; Gates, B. C. The Surface Chemistry of Metal Oxide Clusters: From Metal–Organic Frameworks to Minerals. *ACS Cent. Sci.* **2020**, *6* (9), 1523–1533. https://doi.org/10.1021/acscentsci.0c00803.
- (60) Cavka, J. H.; Jakobsen, S.; Olsbye, U.; Guillou, N.; Lamberti, C.; Bordiga, S.; Lillerud, K. P. A New Zirconium Inorganic Building Brick Forming Metal Organic Frameworks with Exceptional Stability. *J. Am. Chem. Soc.* **2008**, *130* (42), 13850–13851. https://doi.org/10.1021/ja8057953.
- (61) Mondloch, J. E.; Bury, W.; Fairen-Jimenez, D.; Kwon, S.; DeMarco, E. J.; Weston, M. H.; Sarjeant, A. A.; Nguyen, S. T.; Stair, P. C.; Snurr, R. Q.; Farha, O. K.; Hupp, J. T. Vapor-Phase Metalation by Atomic Layer Deposition in a Metal–Organic Framework. *J. Am. Chem. Soc.* **2013**, *135* (28), 10294–10297. https://doi.org/10.1021/ja4050828.
- (62) Furukawa, H.; Gándara, F.; Zhang, Y.-B.; Jiang, J.; Queen, W. L.; Hudson, M. R.; Yaghi, O. M. Water Adsorption in Porous Metal–Organic Frameworks and Related Materials. *J. Am. Chem. Soc.* **2014**, *136* (11), 4369–4381. https://doi.org/10.1021/ja500330a.
- (63) Kim, I. S.; Borycz, J.; Platero-Prats, A. E.; Tussupbayev, S.; Wang, T. C.; Farha, O. K.; Hupp, J. T.; Gagliardi, L.; Chapman, K. W.; Cramer, C. J.; Martinson, A. B. F. Targeted Single-Site MOF Node Modification: Trivalent Metal Loading via Atomic Layer Deposition. *Chem. Mater.* **2015**, *27* (13), 4772–4778. https://doi.org/10.1021/acs.chemmater.5b01560.
- (64) Kung, C.-W.; Mondloch, J. E.; Wang, T. C.; Bury, W.; Hoffeditz, W.; Klahr, B. M.; Klet, R. C.; Pellin, M. J.; Farha, O. K.; Hupp, J. T. Metal–Organic Framework Thin Films as Platforms for Atomic Layer Deposition of Cobalt Ions To Enable Electrocatalytic Water Oxidation. ACS Appl. Mater. Interfaces 2015, 7 (51), 28223–28230. https://doi.org/10.1021/acsami.5b06901.
- (65) Li, Z.; Schweitzer, N. M.; League, A. B.; Bernales, V.; Peters, A. W.; Getsoian, A. "Bean"; Wang, T. C.; Miller, J. T.; Vjunov, A.; Fulton, J. L.; Lercher, J. A.; Cramer, C. J.; Gagliardi, L.; Hupp, J. T.; Farha, O. K. Sintering-Resistant Single-Site Nickel Catalyst Supported by Metal–Organic Framework. *J. Am. Chem. Soc.* 2016, 138 (6), 1977–1982. https://doi.org/10.1021/jacs.5b12515.
- (66) Ikuno, T.; Zheng, J.; Vjunov, A.; Sanchez-Sanchez, M.; Ortuño, M. A.; Pahls, D. R.; Fulton, J. L.; Camaioni, D. M.; Li, Z.; Ray, D.; Mehdi, B. L.; Browning, N. D.; Farha, O. K.; Hupp, J. T.; Cramer, C. J.; Gagliardi, L.; Lercher, J. A. Methane Oxidation to Methanol Catalyzed by Cu-Oxo Clusters Stabilized in NU-1000 Metal–Organic Framework. *J. Am. Chem. Soc.* **2017**, *139* (30), 10294–10301. https://doi.org/10.1021/jacs.7b02936.
- (67) Manna, K.; Ji, P.; Lin, Z.; Greene, F. X.; Urban, A.; Thacker, N. C.; Lin, W. Chemoselective Single-Site Earth-Abundant Metal Catalysts at Metal–Organic Framework Nodes. *Nat Commun* **2016**, *7* (1), 12610. https://doi.org/10.1038/ncomms12610.
- (68) Dan-Hardi, M.; Serre, C.; Frot, T.; Rozes, L.; Maurin, G.; Sanchez, C.; Férey, G. A New Photoactive Crystalline Highly Porous Titanium(IV) Dicarboxylate. *J. Am. Chem. Soc.* **2009**, *131* (31), 10857–10859. https://doi.org/10.1021/ja903726m.
- (69) Feng, X.; Song, Y.; Chen, J. S.; Xu, Z.; Dunn, S. J.; Lin, W. Rational Construction of an Artificial Binuclear Copper Monooxygenase in a Metal–Organic Framework. *J. Am. Chem. Soc.* **2021**, *143* (2), 1107–1118. https://doi.org/10.1021/jacs.0c11920.

- (70) Thompson, A. B.; Pahls, D. R.; Bernales, V.; Gallington, L. C.; Malonzo, C. D.; Webber, T.; Tereniak, S. J.; Wang, T. C.; Desai, S. P.; Li, Z.; Kim, I. S.; Gagliardi, L.; Penn, R. L.; Chapman, K. W.; Stein, A.; Farha, O. K.; Hupp, J. T.; Martinson, A. B. F.; Lu, C. C. Installing Heterobimetallic Cobalt–Aluminum Single Sites on a Metal Organic Framework Support. *Chem. Mater.* 2016, 28 (18), 6753–6762. https://doi.org/10.1021/acs.chemmater.6b03244.
- (71) Desai, S. P.; Ye, J.; Zheng, J.; Ferrandon, M. S.; Webber, T. E.; Platero-Prats, A. E.; Duan, J.; Garcia-Holley, P.; Camaioni, D. M.; Chapman, K. W.; Delferro, M.; Farha, O. K.; Fulton, J. L.; Gagliardi, L.; Lercher, J. A.; Penn, R. L.; Stein, A.; Lu, C. C. Well-Defined Rhodium–Gallium Catalytic Sites in a Metal–Organic Framework: Promoter-Controlled Selectivity in Alkyne Semihydrogenation to *E* -Alkenes. *J. Am. Chem. Soc.* **2018**, *140* (45), 15309–15318. https://doi.org/10.1021/jacs.8b08550.
- (72) Getzler, Y. D. Y. L.; Mahadevan, V.; Lobkovsky, E. B.; Coates, G. W. Synthesis of β-Lactones: A Highly Active and Selective Catalyst for Epoxide Carbonylation. *J. Am. Chem. Soc.* **2002**, *124* (7), 1174–1175. https://doi.org/10.1021/ja017434u.
- (73) Mahadevan, V.; Getzler, Y. D. Y. L.; Coates, G. W. [Lewis Acid]+[Co(CO)4] Complexes: A Versatile Class of Catalysts for Carbonylative Ring Expansion of Epoxides and Aziridines. *Angew. Chem. Int. Ed.* **2002**, *41* (15), 2781–2784. https://doi.org/10.1002/1521-3773(20020802)41:15<2781::AID-ANIE2781>3.0.CO;2-S.
- (74) Bloch, E. D.; Britt, D.; Lee, C.; Doonan, C. J.; Uribe-Romo, F. J.; Furukawa, H.; Long, J. R.; Yaghi, O. M. Metal Insertion in a Microporous Metal—Organic Framework Lined with 2,2'-Bipyridine. *J. Am. Chem. Soc.* **2010**, *132* (41), 14382–14384. https://doi.org/10.1021/ja106935d.
- (75) Wang, C.; Xie, Z.; deKrafft, K. E.; Lin, W. Doping Metal–Organic Frameworks for Water Oxidation, Carbon Dioxide Reduction, and Organic Photocatalysis. *J. Am. Chem. Soc.* **2011**, *133* (34), 13445–13454. https://doi.org/10.1021/ja203564w.
- (76) Gonzalez, M. I.; Bloch, E. D.; Mason, J. A.; Teat, S. J.; Long, J. R. Single-Crystal-to-Single-Crystal Metalation of a Metal-Organic Framework: A Route toward Structurally Well-Defined Catalysts. *Inorg. Chem.* **2015**, *54* (6), 2995–3005. https://doi.org/10.1021/acs.inorgchem.5b00096.
- (77) Song, F.; Wang, C.; Falkowski, J. M.; Ma, L.; Lin, W. Isoreticular Chiral Metal–Organic Frameworks for Asymmetric Alkene Epoxidation: Tuning Catalytic Activity by Controlling Framework Catenation and Varying Open Channel Sizes. *J. Am. Chem. Soc.* **2010**, *132* (43), 15390–15398. https://doi.org/10.1021/ja1069773.
- (78) Feng, D.; Gu, Z.; Li, J.; Jiang, H.; Wei, Z.; Zhou, H. Zirconium-Metalloporphyrin PCN-222: Mesoporous Metal–Organic Frameworks with Ultrahigh Stability as Biomimetic Catalysts. *Angew Chem Int Ed* **2012**, *51* (41), 10307–10310. https://doi.org/10.1002/anie.201204475.
- (79) Feng, D.; Chung, W.-C.; Wei, Z.; Gu, Z.-Y.; Jiang, H.-L.; Chen, Y.-P.; Darensbourg, D. J.; Zhou, H.-C. Construction of Ultrastable Porphyrin Zr Metal—Organic Frameworks through Linker Elimination. *J. Am. Chem. Soc.* **2013**, *135* (45), 17105–17110. https://doi.org/10.1021/ja408084j.
- (80) Feng, D.; Gu, Z.-Y.; Chen, Y.-P.; Park, J.; Wei, Z.; Sun, Y.; Bosch, M.; Yuan, S.; Zhou, H.-C. A Highly Stable Porphyrinic Zirconium Metal—Organic Framework with **Shp-a** Topology. *J. Am. Chem. Soc.* **2014**, *136* (51), 17714–17717. https://doi.org/10.1021/ja510525s.

- (81) Bloch, W. M.; Burgun, A.; Coghlan, C. J.; Lee, R.; Coote, M. L.; Doonan, C. J.; Sumby, C. J. Capturing Snapshots of Post-Synthetic Metallation Chemistry in Metal-Organic Frameworks. *Nature Chem* **2014**, *6* (10), 906–912. https://doi.org/10.1038/nchem.2045.
- (82) Doonan, C. J.; Morris, W.; Furukawa, H.; Yaghi, O. M. Isoreticular Metalation of Metal–Organic Frameworks. *J. Am. Chem. Soc.* **2009**, *131* (27), 9492–9493. https://doi.org/10.1021/ja903251e.
- (83) Ingleson, M. J.; Perez Barrio, J.; Guilbaud, J.-B.; Khimyak, Y. Z.; Rosseinsky, M. J. Framework Functionalisation Triggers Metal Complex Binding. *Chem. Commun.* **2008**, No. 23, 2680. https://doi.org/10.1039/b718367d.
- (84) Rasero-Almansa, A. M.; Corma, A.; Iglesias, M.; Sánchez, F. One-Pot Multifunctional Catalysis with NNN-Pincer Zr-MOF: Zr Base Catalyzed Condensation with Rh-Catalyzed Hydrogenation. *ChemCatChem* **2013**, *5* (10), 3092–3100. https://doi.org/10.1002/cctc.201300371.
- (85) Geary, J.; Aalto, J. P.; Xiao, D. J. Modular Synthesis of Templated Bimetallic Sites in Metal–Organic Framework Pores. *Chem. Mater.* **2024**, *36* (8), 3949–3956. https://doi.org/10.1021/acs.chemmater.4c00500.
- (86) Jeoung, S.; Kim, S.; Kim, M.; Moon, H. R. Pore Engineering of Metal-Organic Frameworks with Coordinating Functionalities. *Coordination Chemistry Reviews* **2020**, 420, 213377. https://doi.org/10.1016/j.ccr.2020.213377.
- (87) Rosi, N. L.; Kim, J.; Eddaoudi, M.; Chen, B.; O'Keeffe, M.; Yaghi, O. M. Rod Packings and Metal-Organic Frameworks Constructed from Rod-Shaped Secondary Building Units. *J. Am. Chem. Soc.* **2005**, *127* (5), 1504–1518. https://doi.org/10.1021/ja0451230.
- (88) Schoedel, A.; Li, M.; Li, D.; O'Keeffe, M.; Yaghi, O. M. Structures of Metal–Organic Frameworks with Rod Secondary Building Units. *Chem. Rev.* **2016**, *116* (19), 12466–12535. https://doi.org/10.1021/acs.chemrev.6b00346.
- (89) Zhu, C.; Xia, Q.; Chen, X.; Liu, Y.; Du, X.; Cui, Y. Chiral Metal–Organic Framework as a Platform for Cooperative Catalysis in Asymmetric Cyanosilylation of Aldehydes. *ACS Catal.* **2016**, *6* (11), 7590–7596. https://doi.org/10.1021/acscatal.6b02359.
- (90) Wang, Z.; Yeary, P.; Feng, X.; Lin, W. Self-Adaptive Metal-Organic Framework Assembles Di-Iron Active Sites to Mimic Monooxygenases. *J. Am. Chem. Soc.* **2023**, *145* (15), 8647–8655. https://doi.org/10.1021/jacs.3c01498.
- (91) Geary, J.; Wong, A. H.; Xiao, D. J. Thermolabile Cross-Linkers for Templating Precise Multicomponent Metal–Organic Framework Pores. *J. Am. Chem. Soc.* **2021**, *143* (27), 10317–10323. https://doi.org/10.1021/jacs.1c04030.
- (92) Lan, G.; Li, Z.; Veroneau, S. S.; Zhu, Y.-Y.; Xu, Z.; Wang, C.; Lin, W. Photosensitizing Metal–Organic Layers for Efficient Sunlight-Driven Carbon Dioxide Reduction. *J. Am. Chem. Soc.* **2018**, *140* (39), 12369–12373. https://doi.org/10.1021/jacs.8b08357.
- (93) Vallee, B. L.; Williams, R. J. Metalloenzymes: The Entatic Nature of Their Active Sites. *Proc. Natl. Acad. Sci. U.S.A.* **1968**, *59* (2), 498–505. https://doi.org/10.1073/pnas.59.2.498.
- (94) Rayder, T. M.; Bensalah, A. T.; Li, B.; Byers, J. A.; Tsung, C.-K. Engineering Second Sphere Interactions in a Host–Guest Multicomponent Catalyst System for the Hydrogenation of Carbon Dioxide to Methanol. *J. Am. Chem. Soc.* **2021**, *143* (3), 1630–1640. https://doi.org/10.1021/jacs.0c08957.
- (95) Xiao, D. J.; Oktawiec, J.; Milner, P. J.; Long, J. R. Pore Environment Effects on Catalytic Cyclohexane Oxidation in Expanded Fe 2 (Dobdc) Analogues. *J. Am. Chem. Soc.* **2016**, *138* (43), 14371–14379. https://doi.org/10.1021/jacs.6b08417.

- (96) Liu, J.; Goetjen, T. A.; Wang, Q.; Knapp, J. G.; Wasson, M. C.; Yang, Y.; Syed, Z. H.; Delferro, M.; Notestein, J. M.; Farha, O. K.; Hupp, J. T. MOF-Enabled Confinement and Related Effects for Chemical Catalyst Presentation and Utilization. *Chem. Soc. Rev.* **2022**, *51* (3), 1045–1097. https://doi.org/10.1039/D1CS00968K.
- (97) Yuan, S.; Feng, L.; Wang, K.; Pang, J.; Bosch, M.; Lollar, C.; Sun, Y.; Qin, J.; Yang, X.; Zhang, P.; Wang, Q.; Zou, L.; Zhang, Y.; Zhang, L.; Fang, Y.; Li, J.; Zhou, H.-C. Stable Metal–Organic Frameworks: Design, Synthesis, and Applications. *Advanced Materials* **2018**, *30* (37), 1704303. https://doi.org/10.1002/adma.201704303.
- (98) Ding, M.; Cai, X.; Jiang, H.-L. Improving MOF Stability: Approaches and Applications. *Chem. Sci.* **2019**, *10* (44), 10209–10230. https://doi.org/10.1039/C9SC03916C.